


Pattern of myocardial ^{99m}Tc -HMDP uptake and impact on myocardial function in patients with transthyretin cardiac amyloidosis

Sarah Pradel, MD,^{a,b} Stéphanie Brun, MD,^{a,b} Gérard Victor, MD,^{c,d} Pierre Pascal, MD,^{b,c} Pauline Fournier, MD,^{a,b} David Ribes, MD,^e Yoan Lavie-Badie, MD,^{a,b,c} Michel Galinier, MD, PhD,^{a,b,d} Didier Carrié, MD, PhD,^{a,b,f} Isabelle Berry, MD, PhD,^{b,c,d} and Olivier Lairez, MD, PhD ^{a,b,c,d} on behalf of the Toulouse Amyloidosis Research Network collaborators

^a Department of Cardiology, Rangueil University Hospital, Toulouse, France

^b Cardiac Imaging Center, Toulouse University Hospital, Toulouse, France

^c Department of Nuclear Medicine, Toulouse University Hospital, Toulouse, France

^d Medical School of Rangueil, University Paul Sabatier, Toulouse, France

^e Department of Nephrology and Organ Transplantation, Rangueil University Hospital, Toulouse, France

^f Medical School of Purpan, University Paul Sabatier, Toulouse, France

Received Mar 20, 2018; accepted May 16, 2018

doi:10.1007/s12350-018-1316-6

Aims. The purpose of the study was to describe the pattern of ^{99m}Tc -labeled phosphate agents myocardial uptake by scintigraphy and explore its impact on left ventricular (LV) functions in transthyretin cardiac amyloidosis (TTR-CA).

Methods. Fifty patients with TTR-CA underwent ^{99m}Tc -hydroxymethylene-diphosphate (^{99m}Tc -HMDP) scintigraphy and echocardiography with measure of LV thickness, longitudinal strain (LS), systolic and diastolic functions. Cardiac retention by scintigraphy was assessed by visual scoring and the heart/whole body (H/WB) ratio was calculated by dividing counts in the heart by counts in late whole-body images.

Results. The mean population age was 79 ± 10 years. Mean H/WB ratio was 12 ± 7 . Myocardial ^{99m}Tc -HMDP uptake on segments 5, 6, 7, 8, 11, 12, 13, 14, 16, and 17 was correlated with H/WB ratio. Mean LVEF and global LS were $51 \pm 10\%$ and $-10 \pm 3\%$, respectively. H/WB ratio was correlated with global LS ($R = 0.408$, $P = .003$), Ea ($R = -0.566$, $P < .001$) and mean left ventricular wall thickness ($R = 0.476$, $P < .001$) but not with LVEF ($R = -0.109$, $P = .453$). Segmental myocardial uptake was slightly correlated with segmental LS ($R = 0.152$, $P < .001$). H/WB ratio was not correlated with NT-proBNP levels ($R = 0.219$, $P = .148$) neither E/Ea ratio ($R = 0.204$, $P = .184$).

Conclusion. These findings show the relationship between bone tracer myocardial uptake and LV functions in patients with TTR cardiac amyloidosis. (J Nucl Cardiol 2020;27:96–105.)

Electronic supplementary material The online version of this article (<https://doi.org/10.1007/s12350-018-1316-6>) contains supplementary material, which is available to authorized users.

The authors of this article have provided a PowerPoint file, available for download at SpringerLink, which summarises the contents of the paper and is free for re-use at meetings and presentations. Search for the article DOI on SpringerLink.com

The collaborators for Toulouse Amyloidosis Research Network group are listed in ‘‘Acknowledgment’’.

Reprint requests: Olivier Lairez, MD, PhD, Department of Cardiology, Rangueil University Hospital, Toulouse, France; lairez@gmail.com 1071-3581/\$34.00

Copyright © 2018 American Society of Nuclear Cardiology.

Key Words: Amyloid heart disease • diseases/processes, SPECT • modalities, image analysis
• technical, others • tracers

Abbreviations

^{99m} Tc-	^{99m} Tc-hydroxymethylene-
HMDP	diphosphonate
H/WB	Heart/whole body
IQR	Inter-quartile range
LV	Left ventricle
LVEF	Left ventricular ejection fraction
LS	Longitudinal strain
NT-proBNP	N-terminal pro-hormone brain natri- uretic peptide
TTR	Transthyretin

See related editorial, pp. 106–108

INTRODUCTION

^{99m}Tc-labeled phosphate agents have a high affinity for transthyretin (TTR)-infiltrated myocardium, allowing a differential diagnosis with light-chain cardiac amyloidosis¹ and other nonamyloidotic left ventricular (LV) hypertrophies.² Pathophysiology of ^{99m}Tc-labeled phosphate agents cardiac depositions by scintigraphy in patients with TTR cardiac amyloidosis remains unclear and the relationship between ^{99m}Tc-labeled phosphate agents uptake and myocardial functions is still unknown. MRI studies have shown that late gadolinium enhancement can have a heterogeneous pattern in the left ventricle.³ Histological studies have shown that late gadolinium enhancement distribution matches the deposition pattern of interstitial amyloid.^{3,4} The relative apical sparing of longitudinal strain (LS) observed in cardiac amyloidosis is associated with relatively less amyloid deposition in the apex than in the base and suggests that regional myocardial function could be impacted differently depending on the localization of protein fibrils deposition.⁴ It was supposed that less extracellular protein deposition lead to less resistance to deformation.⁵ Recent studies have shown that ^{99m}Tc-labeled tracer myocardial pattern is characterized by a base-to-apex gradient with an apical sparing,⁶ which is similar to the apical sparing pattern of LS observed on echocardiography.⁷ Both echocardiographic and scintigraphic apical sparing pattern of LS⁸ and ^{99m}Tc-labeled tracer myocardial uptake,⁷ respectively, have shown prognostic impact in patients with TTR cardiac amyloidosis. Beyond the myocardial distribution, the direct impact of ^{99m}Tc-labeled tracer uptake on myocardial function remains unknown.

The aim of this study was to explore the relationship between cardiac uptake by ^{99m}Tc-hydroxymethylene-diphosphonate (^{99m}Tc-HMDP) scintigraphy and LV functions.

METHODS

Study Population

Consecutive patients referred for cardiac TTR amyloidosis detection by ^{99m}Tc-HMDP were retrospectively screened. Patients with combined visual score 2 or 3 myocardial ^{99m}Tc-HMDP tracer uptake on bone scintigraphy (moderate uptake equal to bone and high uptake greater than bone, respectively) and the absence of a monoclonal protein in serum or urine were considered as positive for TTR cardiac amyloidosis⁹ and were included in the study. Because mild tracer uptake represents a wide variety of amyloidosis⁹ and does not allow reconstruction on tomographic acquisitions, patients with visual score 1 (mild uptake less than bone) were excluded of the study. Because of the sensitivity of bone scintigraphy to myocardial infarction, patients with history of myocardial infarction or coronary artery disease were excluded of the study. Clinical evaluation, cardiovascular risk factors, and medications were then extracted from hospital records.

All patients were informed at the admission that their clinical data could be used for research purpose and gave their consent. The study was approved by our institutional review board.

^{99m}Tc-Hydroxymethylene-Diphosphonate Scintigraphy (^{99m}Tc-HMDP)

All images were acquired on a hybrid dual-head SPECT/CT system (Symbia T6; Siemens Healthcare, Erlangen, Germany) equipped with low-energy, high-resolution collimators 3 hours after injection of 740 MBq of ^{99m}Tc-HMDP intravenously. Acquisitions consisted of whole-body scan (20 cm/minute) in the anterior and posterior views, followed by a tomographic acquisition, consisting of a standard helical CT (120 kV, 100 mAs, slice thickness 2.0 mm, 512 × 512 matrix) for attenuation correction, followed by a SPECT covering the thorax (120 projections, 20 seconds/projection, 128 × 128 matrix).

Image analysis was independently performed by a single blinded observer unaware of clinical and echocardiographic data (GV). Planar images were image analyzed using on the GE Xeleris workstation and visual scoring of cardiac retention was defined as described previously:¹⁰ score 0, absent cardiac uptake and normal bone uptake; score 1, mild cardiac uptake, inferior to bone uptake; score 2, moderate cardiac uptake associated with attenuated bone uptake; or score 3, strong cardiac uptake with mild/absent bone uptake. ^{99m}Tc-HMDP was considered as suggestive of TTR cardiac amyloidosis when the visual score was ≥ 2. Semiquantitative analysis of heart/whole body (H/WB) ratio was then calculated by dividing counts in the heart by counts in late whole-body images after subtracting the activity in the urinary tract and bladder. Quantitative myocardial uptake was performed using the Cedars-Sinai quantitative SPECT protocol from the tomographic images. The tracer uptake was normalized to the brightest point to

give a relative intensity for each of the segments. QPS-derived bull's eye map of regional uptake was generated and then divided into 17 segments. The myocardial uptake values for the six basal, six mid, and five apical segments of the LV were averaged to obtain three 'regional' myocardial uptake values. The apex-to-base gradient in myocardial uptake was examined using a relative apical myocardial uptake which was calculated as follows: relative apical myocardial uptake = (average basal myocardial uptake + mid myocardial uptake)/average apical myocardial uptake.

Echocardiography

All patients underwent a transthoracic echocardiography at the inclusion with a commercially available ultrasound Vivid E9 system (GE Vingmed Ultrasound AS, Horten, Norway) using a 2.5 MHz transducer. A complete M-mode and two-dimensional gray scale echocardiography including the three standard apical views (four, three, and two chambers) using high frame rates (> 60 frames/second) was performed for each patient. All echocardiographic data were synchronized to the electrocardiogram, and acquisition was performed during breath hold.

Image analysis was independently performed by a single blinded observer unaware of clinical and scintigraphic data (SP). For offline 2-dimensional strain imaging, the offline EchoPAC software version 201 (GE Vingmed Ultrasound AS, Horten, Norway) was used. Longitudinal myocardial strain was calculated using speckle tracking from 2D gray-scale images and the automated function imaging technique.¹¹ For the assessment of global longitudinal strain (LS), we calculated the average of the longitudinal systolic peak negative values obtained from the 6 LV segments in the apical 4-, 2-, and 3-chamber views. The results were combined in a single bull's-eye summary, which presented the analysis for each segment using a 17-segment model. The strain values for the six basal, six mid, and five apical segments of the LV were averaged to obtain three 'regional' LS values. The apex-to-base gradient in LS was examined using a relative apical LS which was calculated as follows: relative apical LS = average apical LS/(average basal LS + mid LS).⁵ LV end-diastolic and -systolic volumes and ejection fraction were measured using Simpson's biplane method. The mitral inflow velocity pattern was recorded from the apical 4-chamber view with pulsed-wave Doppler sample volume positioned at the tips of mitral leaflets during diastole. Deceleration time, measured as the distance from peak of the E-wave in the mitral inflow view to the baseline and peak velocities of E and A waves were measured (in patients in sinus rhythm). Mitral annulus lateral Ea velocity was measured by tissue Doppler imaging. All Doppler measurements were made over 3 cardiac cycles and averaged. In patients with atrial fibrillation, the data were averaged over 5 cardiac cycles.

Biochemistry

Renal function was expressed as an estimated glomerular filtration rate, which was calculated according to the modification of diet in renal disease formula. Plasma levels of

N-terminal pro-hormone brain natriuretic peptide (NT-proBNP) were quantified with an electrochemiluminescence immunoassay kit (Elecsys NT-proBNP; Roche Diagnostics, Mannheim, Germany) from venous whole blood samples.

Statistical Analysis

Continuous variables were expressed as mean ± standard deviation. Nominal values were expressed as numbers and percentages. Because NT-proBNP and furosemide dose were not normally distributed, results were presented as median value and interquartile range (IQR). Association between the mean values of continuous variables was compared using the Mann-Whitney rank sum test. Nominal variables were investigated by the Fisher exact test. Mean values of segmental myocardial uptake for the same patient were compared using the Wilcoxon test. Relationships between variables were assessed using Spearman correlation analysis and expressed by *R*. Differences were considered statistically significant for *P*-values of < .05. All analyses were performed using standard statistical software SPSS version 20 (SPSS Inc., Chicago, Illinois).

RESULTS

Baseline Characteristics

Fifty patients were retrospectively included. The mean population age was 79 ± 10 years. Most of the patients (88%) were male. Visual score was 2 and 3 for 23 (46%) and 27 (54%) patients, respectively. Mean H/WB ratio was 12 ± 7. Mean LV ejection fraction (LVEF) and global LS were 51 ± 10% and -10 ± 3%, respectively. No patient had TTR mutation after genetic testing and all patient were considered as wild-type TTR amyloidosis. The population's baseline characteristics are listed in the Table 1.

Pattern of Myocardial ^{99m}Tc-HMDP Uptake

Segmental myocardial ^{99m}Tc-HMDP uptake for the whole population and according to the visual score is presented in Figure 1. Myocardial ^{99m}Tc-HMDP uptake was different between scores 2 and 3 for segments basal anteroseptal (*P* = .02), mid anteroseptal (*P* = .001), mid inferolateral (*P* = .007), apical anterior (*P* = .031), apical septal (*P* = .001), apical inferior (*P* = .012), apical lateral (*P* = .037), and apex (*P* = .036).

Myocardial ^{99m}Tc-HMDP uptake was correlated with H/WB ratio for segments basal inferolateral (*R* = 0.466; *P* = .001), basal anterolateral (*R* = 0.322; *P* = .023), mid anterior (*R* = 0.450; *P* = .001), mid anteroseptal (*R* = 0.455; *P* = .001), mid inferolateral (*R* = 0.462; *P* = .001), mid anterolateral (*R* = 0.321;

Table 1. Population's baseline characteristics

	ATTR n = 50
Age, years	79 ± 10
Male, n (%)	44 (88)
Weight, kg	73 ± 9
Height, m	1.69 ± 0.06
Body mass index, kg/m ²	25.6 ± 2.9
NYHA stage [n (%)]	
I	7 (14)
II	27 (54)
III	13 (26)
IV	3 (6)
Mean	2.2 ± 0.8
Medical history [n (%)]	
Smoking habitus	15 (30)
Hypertension	24 (48)
Diabetes	8 (16)
Hypercholesterolemia	22 (44)
Permanent atrial fibrillation [n (%)]	36 (72)
eGFR (mL/minute)	47 ± 17
Medication at inclusion	
Furosemid [n (%)]	40 (80)
Dose (mg/day) (median [IQR])	80 [40-250]
ACEI or ARB [n (%)]	20 (40)
β-blockers [n (%)]	17 (34)
Calcium channel blockers [n (%)]	9 (18)
Systolic blood pressure, mmHg	124 ± 19
Diastolic blood pressure, mmHg	72 ± 11
Heart rate (beats/min)	72 ± 12
Ejection fraction, %	51 ± 10
Global longitudinal strain, %	- 10 ± 3
H/WB ratio	12 ± 7

ACEI, angiotensin-converting-enzyme inhibitor; ARB, angiotensin II receptor antagonist; eGFR, estimated glomerular filtration rate; IQR, inter-quartile range; H/WB ratio, heart-to-whole body ratio

$P = .023$), apical anterior ($R = 0.468$; $P = .001$), apical septal ($R = 0.541$; $P < .001$), apical lateral ($R = 0.330$; $P = .019$), and apex ($R = 0.329$; $P = .020$). Correlations between myocardial ^{99m}Tc-HMDP uptake and H/WB ratio are presented in Figure 2.

There was a basal to apical gradient for ^{99m}Tc-HMDP uptake: less radionuclide uptake was noted in apical segments as compared to basal and mid segments (Figure 3A). This apical-sparing uptake mimicked the pattern of echocardiographic basal to apical gradient of LS (Figure 3B), but as compared to LS, there was no difference between basal and mid segments for ^{99m}Tc-HMDP uptake. Relative apical myocardial uptake and

LS were 2.7 ± 1.9 and 1.2 ± 0.2 ($P < .001$). There was no correlation between relative apical myocardial ^{99m}Tc-HMDP uptake and relative apical LS ($R = 0.037$, $P = .798$).

Relationship Between Myocardial Tracer Uptake, Left Ventricular Wall Thickness and Left Ventricular Functions

H/WB ratio was correlated with global LS ($R = 0.408$, $P = .003$), mitral Ea lateral velocity ($R = - 0.566$, $P < .001$), and mean LV wall thickness ($R = 0.476$, $P < .001$) but not with LVEF ($R = - 0.109$, $P = .453$; Figure 4). Segmental myocardial ^{99m}Tc-HMDP uptake was slightly correlated with segmental LS ($n = 850$ segments, $R = 0.152$, $P < .001$; Figure 5).

Relationship between Myocardial Tracer Uptake, Natriuretic Peptides, and Left Ventricular Filling Pressures

Among patients with visual score 2 and 3, 16 (70%) and 24 (89%) patients had furosemide, respectively ($P = .089$). There was no difference for furosemide doses among patients with visual score 2 and 3 (80 [IQR 40-188] vs. 100 [IQR 65-310] mg, respectively, $P = .303$). There was no correlation between H/WB ratio and furosemide dose ($R = 0.066$, $P = .683$).

Median NT-proBNP level was 3105 pg/mL [IQR 1748-5413], ranging from 154 to 49,928 pg/mL. H/WB ratio was not correlated with NT-proBNP levels ($R = 0.219$, $P = .148$) neither E/Ea ratio ($R = 0.204$, $P = .184$; Figure 6).

DISCUSSION

This study, using ^{99m}Tc-HMDP scintigraphy, shows that myocardial ^{99m}Tc-labeled phosphate deposition is correlated with the increased LV wall thickness, to the alteration of global and segmental LS, and diastolic dysfunction (as assessed by mitral Ea lateral velocity), while it has no impact on LVEF. Our study confirms previous studies reporting that the ^{99m}Tc-labeled phosphate uptake has a predilection for basal and mid segments, mimicking the pattern of LS by echocardiography.^{6,7} However, our study shows that the correlation between segmental bone tracer myocardial uptake and segmental LS is slight and that the continuous gradient observed from the base to the apex for LS is not fully observed for bone tracer myocardial uptake, for which there is no difference between basal and mid segments. This is confirmed by the absence of correlation between relative apical myocardial ^{99m}Tc-HMDP uptake and relative apical LS. These findings suggest that the

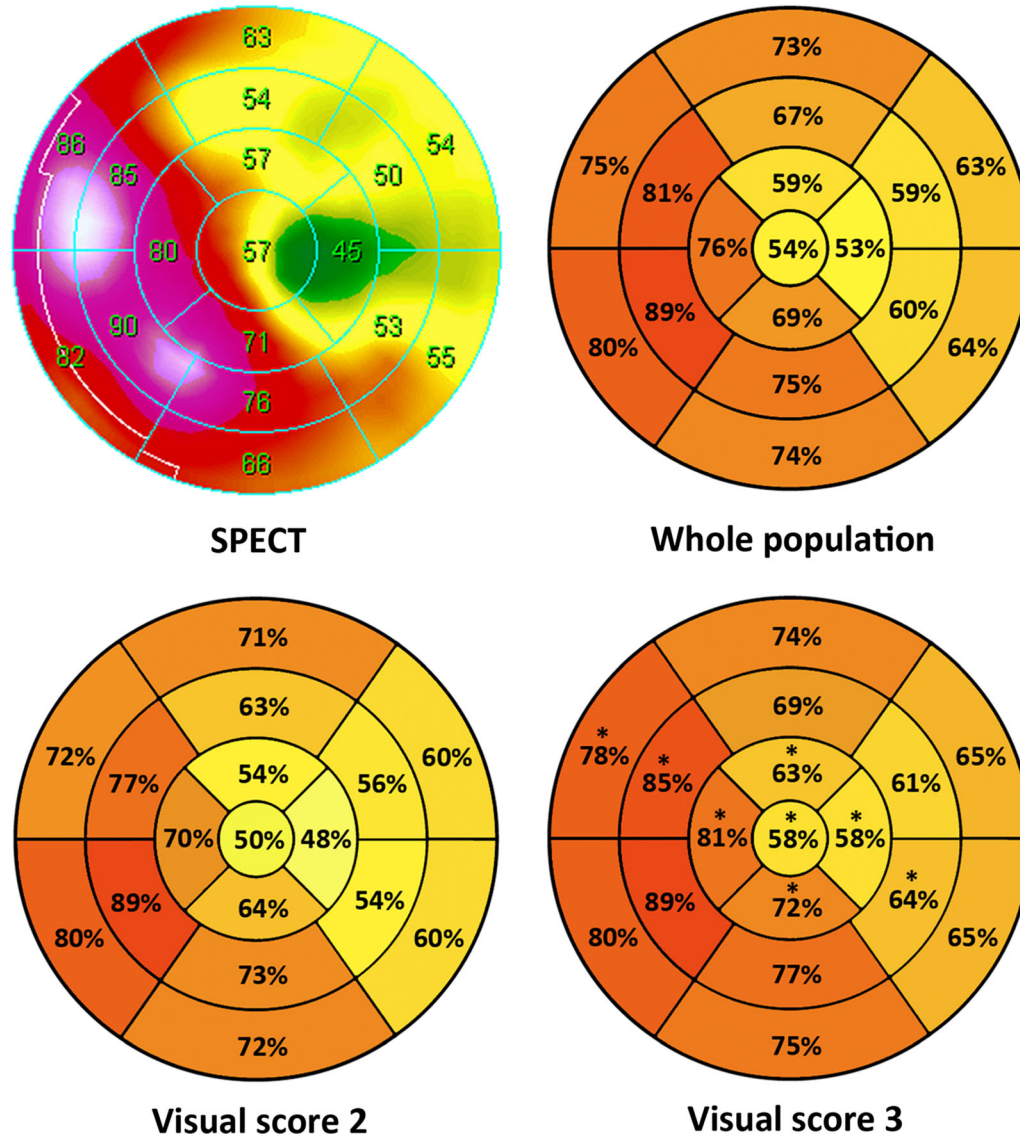


Figure 1. Pattern of myocardial ^{99m}Tc -HMDP uptake. Typical myocardial ^{99m}Tc -HMDP uptake pattern ('bull's eye plot') in patient with transthyretin cardiac amyloidosis (upper left). Representative myocardial ^{99m}Tc -HMDP uptake patterns ('bull's eye plots') in patients with transthyretin cardiac amyloidosis (upper right for whole population, lower left for visual score 2 and lower right for visual score 3). The percentage of maximum activity has been obtained by normalizing the tracer uptake to the brightest point within the left ventricle to give a relative intensity for each of the segments. * P value $< .05$ vs score 2.

mechanisms underlying ^{99m}Tc -labeled tracer myocardial deposition have an impact on LV morphology and function, but this relationship is probably complex and involves other parameters. This could explain the weakness of the correlation between segmental myocardial ^{99m}Tc -HMDP uptake and segmental LS but the statistical strength of the correlation.

Whereas myocardial ^{99m}Tc -labeled phosphate deposition is the consequence of infiltration by TTR fibrils remains to be proven. However, it should be noted that a previous

study has shown that amyloid burden from explanted hearts predominates at the basal level and correlates with LS impairment by echocardiography.⁴ This link between amyloid burden and LS impairment is consistent with our results. The correlation between myocardial ^{99m}Tc -labeled phosphate deposition and LV wall thickening and diastolic dysfunction without impact on LVEF are consistent with the clinical presentation of the disease, which is manifested as a slowly progressive infiltrative cardiomyopathy leading to heart failure with preserved ejection fraction.¹²

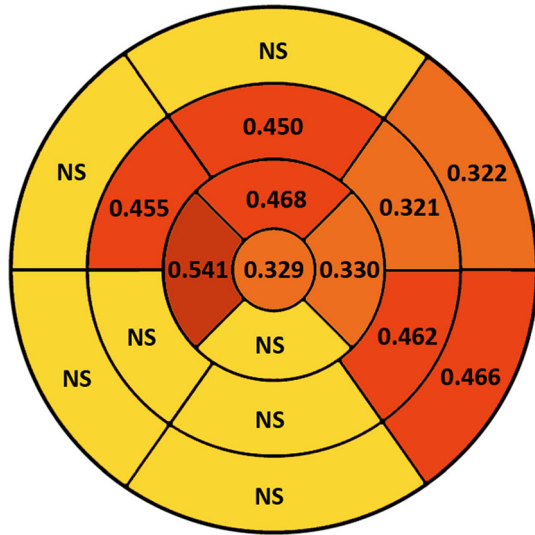


Figure 2. Correlations between heart/whole body ratio and myocardial ^{99m}Tc-HMDP uptake. Bull's eye summarizing part of the myocardium not correlated (yellow) and correlated (orange and red) with the heart/whole body ratio and segmental tracer uptake with the *R*-values for each segmental correlation. *NS* no significant.

Pattern and Intensity of Bone Tracer Myocardial Uptake

Whether all parts of myocardium are affected indifferently by tracer deposition is poorly described. A previous study reported that most of the patients had widespread involvement of all myocardial segments and the septum was all the time involved in the tracer accumulation, which was consistent with the increased

wall thickness.¹ Our study confirms this finding and shows that bone tracer deposition is not homogenous within the whole myocardium: the septum shows a relative greater tracer uptake than the rest of the myocardium.

Because the quantification of segmental myocardial tracer uptake is normalized to the brightest point of the myocardium to give a relative intensity, interpretation of segmental uptake must be made in the light of H/WB ratio. Our study shows that the ^{99m}Tc-labeled phosphate uptake within the myocardium is constant in the basal segments of the anterior and septal walls, and in the inferior wall, whatever the H/WB ratio; whereas it is correlated to H/WB ratio in segments mid anteroseptal, apical septal, mid and apical anterior, basal and mid inferolateral, basal and mid anterolateral, apical lateral, and apex. These findings suggest that some segments are affected differently depending on the overall ^{99m}Tc-HMDP cardiac retention degree, as assessed by H/WB ratio. However, because total myocardial tracer uptake does not significantly change in serial examinations despite clinical progression of the disease,¹³ we cannot establish the link between segmental myocardial involvement and the length of time the pathological process has evolved.

Bone Tracer Deposition and Myocardial Function

The amyloid deposits disrupt the structure of the myocardium, both via progressive clogging of the interstitial space and via direct cytotoxic effects.¹⁴ It

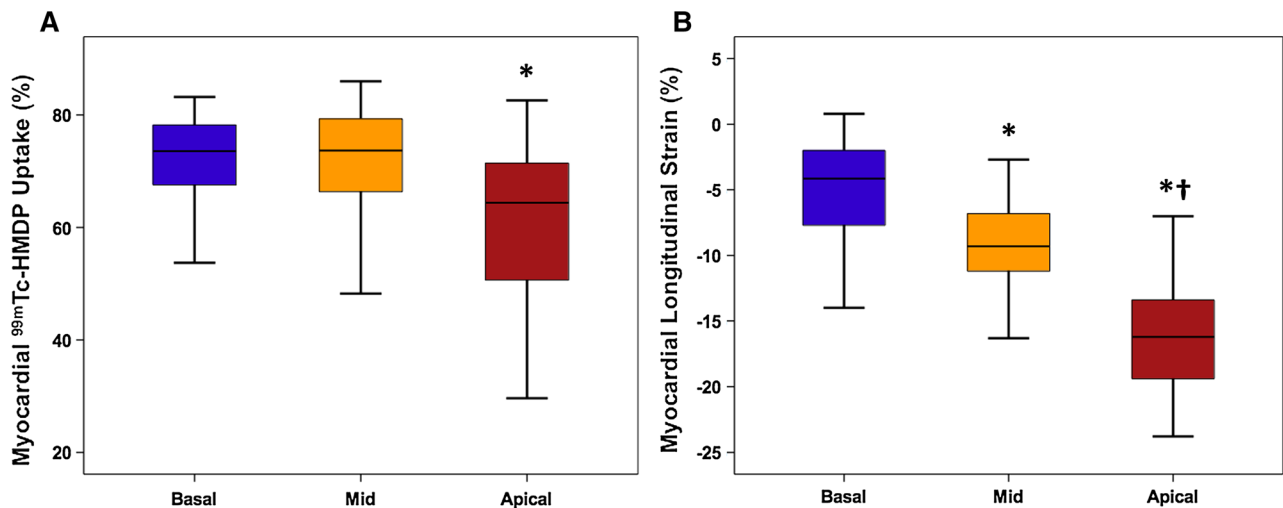


Figure 3. Box plots of ^{99m}Tc-HMDP uptake and echocardiographic longitudinal strain. **A** Segmental analyses of ^{99m}Tc-HMDP uptake and **B** echocardiographic longitudinal strain. There is a basal to apical gradient of decreasing ^{99m}Tc-HMDP uptake and improved longitudinal strain. **P* < .001 vs. basal segments. †*P* < .001 vs. mid segments.

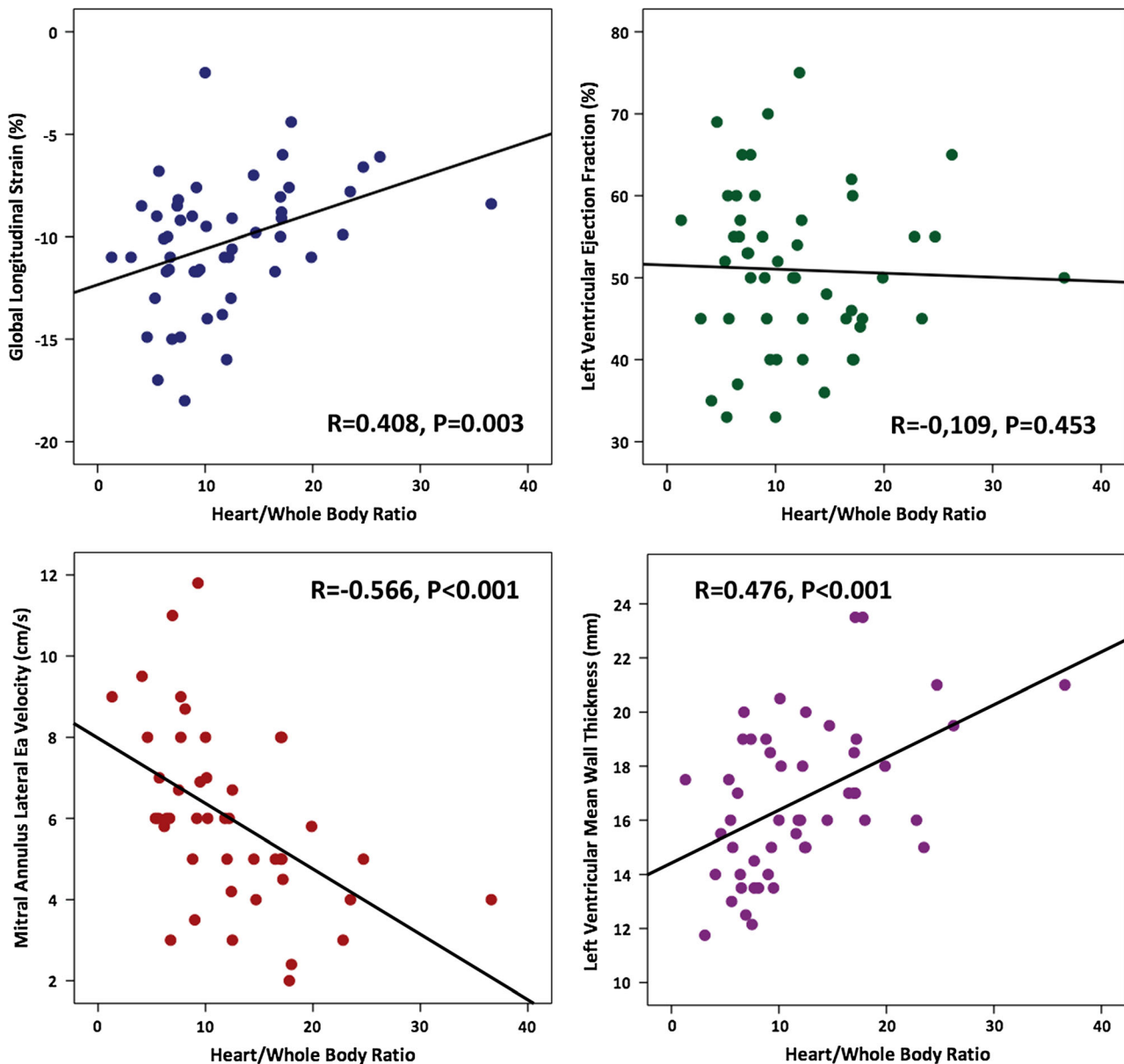


Figure 4. Relationship between heart/whole body ratio, left ventricular function and left ventricular mean wall thickness.

has been suggested that an early consequence of extracellular myocardial amyloid deposition is impaired diastolic ventricular filling.¹⁵ Thickening of the LV wall and diastolic dysfunction are commonly present in cardiac amyloidosis: both early and late cardiac amyloidosis show reduced diastolic velocities.¹⁶ With progression of the disease, more extensive amyloid deposits are supposed to cause atrophy of myocardial cells with attendant reduction of systolic function. In the later stages, there is fibrosis and collagen deposition, which further impairs the diastolic and systolic performance of the ventricle.¹⁷ Reduced systolic function, as

measured by low ejection fraction, is uncommon until the more severe stages of disease.¹⁸ This interaction between amyloid burden and LV morphology and functions mimics the correlation reported in our study between ^{99m}Tc -labeled phosphate myocardial uptake, as assessed by H/WB ratio, and LV wall thickness, diastolic dysfunction, as demonstrated by the decrease of mitral annulus Ea velocity and contractility impairment, as demonstrated by the alteration of global LS. Previous studies have reported a correlation between ^{99m}Tc -labeled phosphate agents heart retention and LV wall thickness.^{10,19} One of them found that H/WB ratio

was inversely correlated with LVEF.¹⁹ Our findings confirm that reduced ejection fraction is uncommon until the more severe stages of disease and impairment in LS occur before ejection fraction becomes abnormal.¹⁸ All these findings, and the recent study reporting the link between amyloid burden and LS impairment,⁴ suggest that there is a link between ^{99m}Tc-labeled phosphate deposition and extracellular TTR fibrils deposition. Fibrosis and collagen deposition, unrelated to bone tracer uptake, and the evolution of the disease on

its own, regardless of the amyloid charge, would explain that total myocardial tracer uptake does not significantly change in serial examinations despite clinical progression of the disease.¹³

Bone Tracer Deposition and Ventricular Filling Pressure

The natural history of interstitial deposition of cardiac TTR causes increased chamber stiffness and intraventricular pressure, followed by decreased systolic function. E/Ea ratio is considered an indication of diastolic dysfunction and increased pressure,²⁰ and was proposed to unmask subclinical increase of LV filling pressure in patients with cardiac amyloidosis and normal ejection fraction.²¹ Assuming that the degree of myocardial ^{99m}Tc-labeled phosphate deposition is related to the amyloid burden, it is surprising that we do not find correlation between ^{99m}Tc-labeled phosphate tracer and NT-proBNP levels or E/Ea ratio. However, a recent autopsy study showed that wild-type amyloid TTR deposition within the myocardium is associated with age and is common after 65-year-old, even in the absence of symptoms.²² The presence of TTR deposits in the absence of symptoms suggests that amyloid deposition is not necessarily accompanied by an increase in ventricular filling pressure. The increased chamber stiffness in patients with cardiac amyloidosis shifts up the resting diastolic pressure–volume relationship and increases sensitivity to changes in blood volume, which could participate to the high variability of ventricular filling pressure and the lack of correlation with ^{99m}Tc-

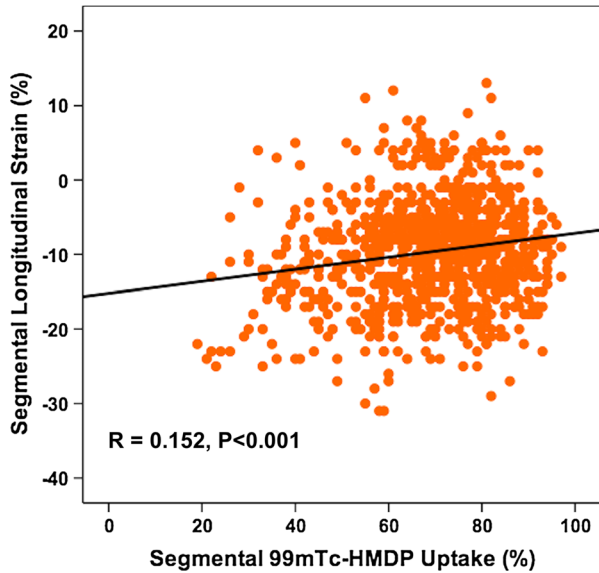


Figure 5. Correlation between segmental tracer uptake and segmental left ventricular longitudinal strain.

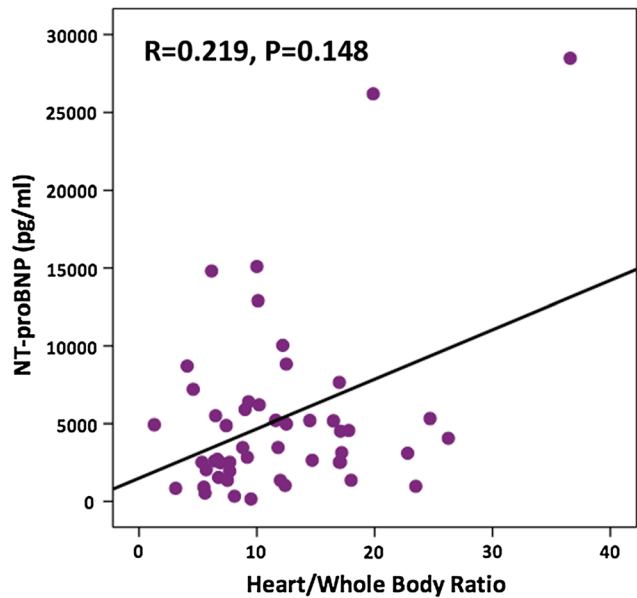
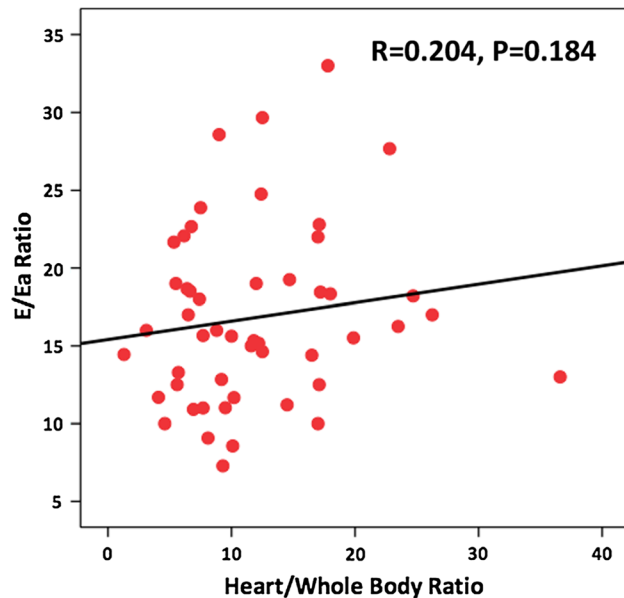


Figure 6. Relationship between heart/whole body ratio and left ventricular filling pressures.

labeled phosphate deposition. Indeed, filling pressures are dynamic, highly variable and dependent on multiple factors, which could explain this lack of correlation. Furthermore, it is important to note that elevation of NT-proBNP levels in cardiac amyloidosis may be due not only to elevated ventricular filling pressure but also to direct myocytes damage due to extracellular deposits of amyloid.²³

Limitations

The Cedar's Sinai QGS software has not been validated for myocardial HMDP uptake quantification. However, it is widely used for myocardial perfusion tracer uptake quantification. Myocardial HMDP uptake quantification could be different than myocardial perfusion tracer uptake quantification since we cannot exclude a residual circulating activity within the left ventricle. However, we used the late-phase images (i.e., images obtained after 3 hours of circulating time), and considered that there was no residual circulating activity.

Whether TTR amyloid deposits affect cardiac function in the same way than other amyloid proteins remain unknown, and our results can only be interpreted in the context of wild-type TTR amyloidosis.

Finally, our study has all the limitations associated with retrospective and single-site studies. We can suppose that site experience and imaging protocol could impact the validity of our results.

CONCLUSION

Myocardial ^{99m}Tc-labeled phosphate deposition is correlated with the increased LV wall thickness and leads to the alteration of global and segmental LS, and diastolic dysfunction in patients with wild-type TTR amyloidosis. Whereas the basal segments are affected independently of total myocardial bone tracer deposition, anterior and lateral walls, and apex, appear to depend on total bone tracer uptake. These findings suggest that bone tracer myocardial uptake could be linked to amyloid burden.

Toulouse Amyloidosis Research Network collaborators

Stanislas Faguer, MD, PhD, Dominique Chauveau, MD, PhD, Antoine Huart, MD, Joelle Guitard, MD, Pauline Bernadet Monrozies, MD (Department of Nephrology and Referral Center for Rare Diseases, University Hospital of Rangueil, Toulouse, France); Pascal Cintas, MD, PhD (Department of Neurology, Purpan University Hospital, Toulouse, France); Laurent Alric, MD, PhD (Department of

Internal Medicine and Digestive Diseases, Purpan University Hospital, Toulouse, France); Daniel Adoue, MD, PhD, Laurent Sailler, MD, PhD, Leonardo Astudillo, MD (Department of Internal Medicine, Toulouse University Hospital, Toulouse, France); Bénédicte Puissant, MD (Immunology Laboratory, Toulouse University Hospital, Toulouse, France); Grégoire Prévot, MD (Department of Pneumology, Toulouse University Hospital, Toulouse, France); Magali Colombat, MD, PhD, Audrey Delas, MD (Department of Pathology, IUCT Oncopôle, Toulouse, France); Murielle Roussel, MD (Department of Hematology, Toulouse University Hospital, Toulouse, France); Eve Cariou, MD (Department of Cardiology, Rangueil University Hospital, Toulouse, France); Delphine Dupin-Deguine, MD.

Disclosure

The authors have no conflict of interest to disclose.

References

1. Perugini E, Guidalotti PL, Salvi F, et al. Noninvasive etiologic diagnosis of cardiac amyloidosis using 99 mTc-3,3-diphosphono-1,2-propanodicarboxylic acid scintigraphy. *J Am Coll Cardiol* 2005;46:1076-84.
2. Quarta CC, Guidalotti PL, Longhi S, et al. Defining the diagnosis in echocardiographically suspected senile systemic amyloidosis. *JACC Cardiovasc Imaging* 2012;5:755-8.
3. Syed IS, Glockner JF, Feng D, et al. Role of cardiac magnetic resonance imaging in the detection of cardiac amyloidosis. *JACC Cardiovasc Imaging* 2010;3:155-64.
4. Ternacle J, Bodez D, Guellich A, et al. Causes and consequences of longitudinal LV dysfunction assessed by 2D strain echocardiography in cardiac amyloidosis. *JACC Cardiovasc Imaging* 2016;9:126-38.
5. Phelan D, Collier P, Thavendiranathan P, et al. Relative apical sparing of longitudinal strain using two-dimensional speckle-tracking echocardiography is both sensitive and specific for the diagnosis of cardiac amyloidosis. *Heart* 2012;98:1442-8.
6. Van Der Gucht A, Cottreau A-S, Abulizi M, et al. Apical sparing pattern of left ventricular myocardial (99 m)Tc-HMDP uptake in patients with transthyretin cardiac amyloidosis. *J Nucl Cardiol* 2017. <https://doi.org/10.1007/s12350-017-0894-z>.
7. Sperry BW, Vranian MN, Tower-Rader A, et al. Regional variation in technetium pyrophosphate uptake in transthyretin cardiac amyloidosis and impact on mortality. *JACC Cardiovasc Imaging* 2018;11:234-42.
8. Senapati A, Sperry BW, Grodin JL, et al. Prognostic implication of relative regional strain ratio in cardiac amyloidosis. *Heart* 2016;102:748-54.
9. Gillmore JD, Maurer MS, Falk RH, et al. Nonbiopsy diagnosis of cardiac transthyretin amyloidosis. *Circulation* 2016;133:2404-12.
10. Rapezzi C, Quarta CC, Guidalotti PL, et al. Usefulness and limitations of 99 mTc-3,3-diphosphono-1,2-propanodicarboxylic acid scintigraphy in the aetiological diagnosis of amyloidotic cardiomyopathy. *Eur J Nucl Med Mol Imaging* 2011;38:470-8.
11. Voigt J-U, Pedrizzetti G, Lysyansky P, et al. Definitions for a common standard for 2D speckle tracking echocardiography: Consensus document of the EACVI/ASE/Industry Task Force to standardize deformation imaging. *Eur Heart J Cardiovasc Imaging* 2015;16:1-11.

12. Gertz MA, Benson MD, Dyck PJ, et al. Diagnosis, prognosis, and therapy of transthyretin amyloidosis. *J Am Coll Cardiol* 2015;66:2451-66.
13. Castano A, DeLuca A, Weinberg R, et al. Serial scanning with technetium pyrophosphate ((99 m)Tc-PYP) in advanced ATTR cardiac amyloidosis. *J Nucl Cardiol* 2016;23:1355-63.
14. Damy T, Jaccard A, Guellich A, et al. Identification of prognostic markers in transthyretin and AL cardiac amyloidosis. *Amyloid Int J Exp Clin Investig Off J Int Soc Amyloidosis* 2016;23:194-202.
15. Swanton RH, Brooksby IA, Davies MJ, et al. Systolic and diastolic ventricular function in cardiac amyloidosis. Studies in six cases diagnosed with endomyocardial biopsy. *Am J Cardiol* 1977;39:658-64.
16. Koyama J, Ray-Sequin PA, Davidoff R, Falk RH. Usefulness of pulsed tissue Doppler imaging for evaluating systolic and diastolic left ventricular function in patients with AL (primary) amyloidosis. *Am J Cardiol* 2002;89:1067-71.
17. Wizenberg TA, Muz J, Sohn YH, et al. Value of positive myocardial technetium-99m-pyrophosphate scintigraphy in the noninvasive diagnosis of cardiac amyloidosis. *Am Heart J* 1982;103:468-73.
18. Selvanayagam JB, Hawkins PN, Paul B, et al. Evaluation and management of the cardiac amyloidosis. *J Am Coll Cardiol* 2007;50:2101-10.
19. Rapezzi C, Quarta CC, Guidalotti PL, et al. Role of (99m)Tc-DPD scintigraphy in diagnosis and prognosis of hereditary transthyretin-related cardiac amyloidosis. *JACC Cardiovasc Imaging* 2011;4:659-70.
20. Nagueh SF, Smiseth OA, Appleton CP, et al. Recommendations for the evaluation of left ventricular diastolic function by echocardiography: An update from the American Society of Echocardiography and the European Association of Cardiovascular Imaging. *Eur Heart J Cardiovasc Imaging* 2016;17:1321-60.
21. Schiano-Lomoriello V, Galderisi M, Mele D, et al. Longitudinal strain of left ventricular basal segments and E/e' ratio differentiate primary cardiac amyloidosis at presentation from hypertensive hypertrophy: an automated function imaging study. *Echocardiography* 2016;33:1335-43.
22. Mohammed SF, Mirzoyev SA, Edwards WD, et al. Left ventricular amyloid deposition in patients with heart failure and preserved ejection fraction. *JACC Heart Fail* 2014;2:113-22.
23. Nordlinger M, Magnani B, Skinner M, Falk RH. Is elevated plasma B-natriuretic peptide in amyloidosis simply a function of the presence of heart failure? *Am J Cardiol* 2005;96:982-4.